



## Sorption of ammonium and phosphate from aqueous solution by biochar derived from phytoremediation plants\*

Zheng ZENG<sup>§1</sup>, Song-da ZHANG<sup>§1,2</sup>, Ting-qiang LI<sup>1</sup>, Feng-liang ZHAO<sup>1</sup>, Zhen-li HE<sup>3</sup>, He-ping ZHAO<sup>†‡1</sup>,  
 Xiao-e YANG<sup>†‡1</sup>, Hai-long WANG<sup>4</sup>, Jing ZHAO<sup>1</sup>, Muhammad Tariq RAFIQ<sup>1</sup>

<sup>(1)</sup>Ministry of Education Key Laboratory of Environmental Remediation and Ecological Health,  
 College of Environmental and Resource Sciences, Zhejiang University, Hangzhou 310058, China)

<sup>(2)</sup>Ningbo Raw Water Group Co., Ltd., Ningbo 315100, China)

<sup>(3)</sup>Indian River Research and Education Center, Institute of Food and Agricultural Sciences,  
 University of Florida, Fort Pierce, FL 34945, USA)

<sup>(4)</sup>School of Environmental and Resource Sciences, Zhejiang A&F University, Lin'an 311300, China)

<sup>†</sup>E-mail: hopechoil@gmail.com; xyang@zju.edu.cn

Received Apr. 5, 2013; Revision accepted July 29, 2013; Crosschecked Nov. 20, 2013

**Abstract:** The study on biochar derived from plant biomass for environmental applications is attracting more and more attention. Twelve sets of biochar were obtained by treating four phytoremediation plants, *Salix rosthornii* Seemen, *Thalia dealbata*, *Vetiveria zizanioides*, and *Phragmites* sp., sequentially through pyrolysis at 500 °C in a N<sub>2</sub> environment, and under different temperatures (500, 600, and 700 °C) in a CO<sub>2</sub> environment. The cation exchange capacity and specific surface area of biochar varied with both plant species and pyrolysis temperature. The magnesium (Mg) content of biochar derived from *T. dealbata* (TC) was obviously higher than that of the other plant biochars. This biochar also had the highest sorption capacity for phosphate and ammonium. In terms of biomass yields, adsorption capacity, and energy cost, *T. dealbata* biochar produced at 600 °C (TC600) is the most promising sorbent for removing contaminants (N and P) from aqueous solution. Therefore, *T. dealbata* appears to be the best candidate for phytoremediation application as its biomass can make a good biochar for environmental cleaning.

**Key words:** Biochar, Nutrient removal, Plant species, Pyrolysis temperature, Water quality

doi:10.1631/jzus.B1300102

Document code: A

CLC number: X52

### 1 Introduction

It is well known that increased nitrogen (N) and phosphorus (P) inputs have resulted in accelerated water eutrophication worldwide (Conley *et al.*, 2009).

Eutrophication in lakes, reservoirs, estuaries, and rivers is a common environmental issue, especially in developing countries like China (Yang *et al.*, 2008). Thus, cost-effective and highly efficient water treatment technologies are desirable. Constructed wetlands have emerged as a promising approach owing to their bioremediation potential. Both terrestrial and aquatic plants have been utilized to remove N and P from wastewater (Abe and Ozaki, 1998). Plants like *Thalia dealbata*, *Vetiveria zizanioides*, and *Phragmites* sp. are widely used in constructed wetlands for eutrophication control (Valipour *et al.*, 2009; Zhao *et al.*, 2012). Seo *et al.* (2010) examined the nitrate and phosphate removal potential of three *Salix* species in a

<sup>‡</sup> Corresponding authors

<sup>§</sup> The two authors contributed equally to this work

\* Project supported by the International Cooperative Project from the Ministry of Science and Technology of China (No. 2010DFB33960), the National Key Technology R&D Program of China (No. 2012BAC17B02), the Zhejiang Youth Creative Program (No. 2012QNA6004), and the Key Project from Zhejiang Science and Technology Bureau (No. 2011C13015), China

© Zhejiang University and Springer-Verlag Berlin Heidelberg 2013

eutrophic aquatic environment, and found that rose-gold pussy willow is best for N removal, and the highest P removal was observed in giant pussy willow. However, if these wetland plants are not harvested properly, nutrients that have been taken up by plants will be released back into the water during the decomposition processes (Brix, 1997; Lu *et al.*, 2010). Thus, harvesting the plants and subsequent processing are critical. Harvested plant biomass can be used as soil amendment, processed into livestock feed (Valix *et al.*, 2004; Cao and Harris, 2010; Lu *et al.*, 2010), or converted into usable energy through other pathways. In China, plant energy research has focused mostly on bioethanol and biogas production (Wilkie and Evans, 2010).

Biomass is one of the largest sustainable energy sources in the world. The utilization of biomass for energy production has gained increasing popularity in some countries (Karaosmanoglu *et al.*, 2000) because it can reduce the risk of energy shortage. Biochar is a pyrogenic carbon-rich material produced from waste biomass, in particular agricultural wastes such as corn, sugarcane bagasse, and peanuts (Kameyama *et al.*, 2011; Yuan *et al.*, 2011). Many studies have evaluated the use of biochar as adsorbents for the removal of heavy metals, pathogens, and other pollutants in wastewater. Xu *et al.* (2013) showed that biochar derived from dairy manure was effective for removing heavy metals, e.g., Pb, Cu, Zn, or Cd, from wastewater. Mohan *et al.* (2007) found that oak bark char could significantly remove  $Pb^{2+}$  and  $Cd^{2+}$ . Chun *et al.* (2004) reported that crop residue-derived chars in agricultural soils served as a potential medium for retaining organic contaminants. However, research on nutrient removal, particularly ammonium and phosphate from water by biochar, is limited (Hossain *et al.*, 2011; Yao *et al.*, 2011a).

In this study, we investigated ammonium and phosphate sorption by selective biochar derived from four phytoremediation plants, *Salix rosthornii* Seemen, *T. dealbata*, *V. zizanioides*, and *Phragmites* sp., which were subjected to different temperatures (500, 600, and 700 °C) through slow pyrolysis. Our objectives were to compare the physicochemical characteristics of biochars derived at different temperatures and to evaluate the potential of pyrolyzed biochar for ammonium and phosphate removal from aqueous solution.

## 2 Materials and methods

### 2.1 Materials and preparation

The biochar samples used in this study were produced from four plants: *S. rosthornii* Seemen, *T. dealbata*, *V. zizanioides*, and *Phragmites* sp. *S. rosthornii* was collected from the Huajiachi Campus, Zhejiang University, China. The other three plants were collected from the Qingshanhu constructed wetland, Lin'an, China. The plants were air-dried in a greenhouse for 7 d, and then ground and passed through a 1-mm sieve. The powder was dried at 105 °C for 24 h prior to carbonization and activation treatment.

**Carbonization:** Biochar powder was first pyrolyzed to 500 °C in a furnace (KBF11Q, Zhengguang, China) under  $N_2$  atmosphere at a ramp rate of 5 °C/min and incubated at the peak temperature for 2 h before cooling down to room temperature.

**Activation:** Four types of carbonized biochar were further pyrolyzed to three different temperatures (500, 600, and 700 °C) in  $CO_2$  atmosphere under the same conditions (heating rate of 5 °C/min for 2 h).

The resulting biochars were cooled to room temperature in the  $CO_2$  atmosphere. Twelve products were obtained (Table 1): SC500, SC600, SC700 (*S. rosthornii* Seemen), TC500, TC600, TC700 (*T. dealbata*), VC500, VC600, VC700 (*V. zizanioides*), PC500, PC600, and PC700 (*Phragmites* sp.).

### 2.2 Biochar properties

Elemental CHN analyses were performed using a CHN elemental analyzer (Flash-EA112, Thermo Finnigan). Available P was determined by the Olsen method using an ultraviolet spectrophotometer (Lambda 35, PerkinElmer). Ca, Mg, Fe, and Al were measured by inductively coupled plasma mass spectrometry (ICP-MS; 7500a, Agilent). The cation exchange capacity (CEC) was measured by the method of Schollenberger and Simon (1945).

Fourier transform infrared (FTIR) analysis (Nicolet 6700) of the biochar was performed to identify the surface functional groups. The biochars were analyzed by infrared spectroscopy between 400 and 4000  $cm^{-1}$ , with 50 scans being taken at 2  $cm^{-1}$  resolution. Scanning electron microscopy (SEM; SU1510, Hitachi) was used to compare the structures and surface characteristics of the four biochar samples. The pH of the biochar was measured by adding

biochar to deionized water at a mass/water ratio of 1:20 (Inyang *et al.*, 2012). The solution was then manually shaken and allowed to stand for 5 min before the pH was measured.

The specific surface area of biochar was determined by N<sub>2</sub> adsorption isotherms at 77 K and by CO<sub>2</sub> isotherms at 273 K using a Quadrasorb Si-MP surface area analyzer, N<sub>2</sub> adsorption isotherms at 77 K using the Brunauer-Emmett-Teller (BET) method for mesopore-enclosed surfaces and CO<sub>2</sub> adsorption isotherms at 273 K using grand canonical Monte Carlo simulations of non-local density functional theory (NLDFT) for micropore-enclosed (<1.5 nm) surfaces (Yao *et al.*, 2011a; Inyang *et al.*, 2012).

### 2.3 Sorption experiments

Ammonium and phosphate solutions were prepared by dissolving NH<sub>4</sub>Cl and K<sub>2</sub>HPO<sub>4</sub> in deionized water. Adsorption isotherms of ammonium and phosphate from their individual solutions were determined using batch experiments in triplicate. A total of 0.2 g adsorbent was added to 50 ml of ammonium or phosphate solution. The initial pH for each sorption solution was adjusted to 7 prior to the sorption experiments. The vessels were shaken at 200 r/min in a mechanical shaker for 24 h at room temperature, and the final suspensions were centrifuged, filtered, and stored at room temperature until analysis. The sorbed amount was calculated from the difference between the initial and final concentrations of the nutrient in the solution.

To evaluate the sorption capacity for environmental treatment, removal rates of ammonium and phosphate were measured with 0.2 g of each adsorbent added into 30 mg N/L and 30 mg P/L solutions, respectively. Removal rates were calculated based on the initial and final aqueous concentrations.

### 2.4 Statistical analysis

The data of sorption of ammonium and phosphate were described by analyses of regression. Other statistical analyses were conducted using the programs of Origins 8.0. The error bars represent standard deviation (SD), calculated from triplicate data.

## 3 Results and discussion

### 3.1 Biochar characterization

Biochar yield decreased with increasing pyrolysis temperature (Table 1). The biochar yields of the four plant biomasses SC, TC, VC, and PC were 24.48%–27.62%, 22.81%–31.98%, 28.21%–31.51%, and 29.32%–33.59%, respectively, when activated at different temperatures. These production rates are comparable, or greater than commonly used plant materials such as olive husk and corncob produced at the same temperatures (Demirbas, 2004). Therefore, the biomasses of the four plant species can be good candidates for biochar feedstock.

**Table 1** Physicochemical properties of biochar derived from four plants under different pyrolysis temperatures

Biochar	Temp. (°C)	pH	Yield (%)	CEC (mmol/kg)	Surface area (m <sup>2</sup> /g)		C (%)	H (%)	N (%)	Available P (g/kg)	Ca (g/kg)	Mg (g/kg)	Fe (g/kg)	Al (g/kg)
					N <sub>2</sub>	CO <sub>2</sub>								
SC500	500	10.77	27.62	234.7	243.77	361.81	75.35	2.63	1.27	0.65	20.18	0.94	0.44	0.32
SC600	600	10.80	26.84	118.3	324.25	399.98	83.61	2.26	1.26	0.48	20.52	1.19	0.40	0.30
SC700	700	10.89	24.48	61.4	448.29	495.62	84.60	1.66	1.28	0.42	21.69	1.43	0.46	0.36
TC500	500	10.39	31.98	312.3	3.57	114.11	75.08	2.59	3.43	1.56	18.34	3.57	0.59	0.32
TC600	600	10.49	31.08	288.2	17.53	287.95	74.48	2.02	2.98	1.74	18.10	3.43	0.42	0.29
TC700	700	10.64	22.81	195.7	223.08	228.33	57.08	2.21	2.31	3.11	19.66	4.42	0.64	0.44
VC500	500	10.27	31.51	210.7	83.01	354.13	77.66	2.77	1.62	0.84	16.51	1.49	0.86	0.78
VC600	600	10.56	30.60	157.1	266.23	401.44	82.15	2.23	1.82	0.34	17.04	1.57	0.90	0.74
VC700	700	10.74	28.21	143.6	362.27	483.12	83.29	1.67	1.85	0.42	17.99	1.51	0.82	0.68
PC500	500	10.20	33.59	218.0	107.82	287.51	66.92	2.42	4.10	0.83	18.18	1.65	0.52	0.40
PC600	600	10.35	33.52	129.4	226.25	341.24	69.33	1.83	3.42	0.56	18.28	1.72	0.54	0.53
PC700	700	10.98	29.32	172.4	301.24	424.63	66.66	1.45	3.05	0.79	19.47	1.79	0.59	0.44

SC: *S. rosthornii* Seemen; TC: *T. dealbata*; VC: *V. zizanioides*; PC: *Phragmites* sp.; CEC: cation exchange capacity

CHN analysis revealed that for the same biochar material, as the activation temperature increased, the yield rate gradually decreased because of the degradation of remaining carbonized material. Carbon contents generally increased, whereas H and O contents decreased with increasing activation temperature, indicating an increased degree of carbonization of the biochar (Chun *et al.*, 2004). However, the C content of TC700 decreased along with the increasing temperature, probably because more ash is produced at higher temperatures. The Ca content of all biochar was similar, regardless of temperature, but TC had a high content of available P and Mg, approximately three times greater than the other biochar. It is likely *T. dealbata* has a greater capacity for uptake and accumulation of P and Mg.

Surface areas generally increased with increasing temperature. Although N<sub>2</sub> is widely used as a standard probe gas for surface area measurement, N<sub>2</sub> is unable to reach the internal microporosity associated with materials such as biochar, kerogen, and humic substances (Pignatello *et al.*, 2006). The surface area determined by CO<sub>2</sub> was higher than that determined by N<sub>2</sub> because CO<sub>2</sub> diffuses more easily at 273 K and has a smaller molecular size than N<sub>2</sub> (Pignatello *et al.*, 2006). The BET method relies on several assumptions that may not be true for microporous materials with very narrow pores and ultra-high surface areas (Walton and Snurr, 2007). The modern approach, which involves the application of NLDFT, provides a more reliable size analysis of

both micropores and mesopores (Ravikovitch and Neimark, 2001). Therefore, the CO<sub>2</sub> (NLDFT) method should be more adequate for determining the surface area of biochar (Pignatello *et al.*, 2006; Yao *et al.*, 2011a). Biochar (SC, PC, and VC) and TC700 had a large N<sub>2</sub> surface area, indicating the presence of mesopores (Yao *et al.*, 2011a). The N<sub>2</sub>-determined surface areas of TC500 (3.57 m<sup>2</sup>/g) and TC600 (17.53 m<sup>2</sup>/g) were much lower than the corresponding CO<sub>2</sub>-determined values (114.11 and 287.95 m<sup>2</sup>/g), indicating that TC500 and TC600 have been dominated by micropores. TC600 had a larger surface area than TC500, for more micropores of TC were developed with increasing temperature, while TC700 has some mesopores because the high temperature destroyed the microstructure.

The infrared spectra of the adsorbents (Fig. 1) revealed their complex chemical bonding consisting of different organic structures. The spectra of SC600, VC600, and PC600 were of similar shapes (aromatic C=O, C=C 1616 cm<sup>-1</sup>, -CH<sub>2</sub>- 1400 cm<sup>-1</sup>, CO and CC stretching 1117 cm<sup>-1</sup>, and furan γ-CH 875 cm<sup>-1</sup>), but were different from the TC600 spectrum, which had more peaks, e.g., the aliphatic C-O-C functional groups of cellulose at 1043 cm<sup>-1</sup> and carbohydrate C-O at 990 cm<sup>-1</sup> (Uchimiya *et al.*, 2010; Kumar *et al.*, 2011). The bands for aliphatic CH<sub>2</sub> groups in TC600 at 1440 and 1400 cm<sup>-1</sup> indicate that TC600 has more nonpolar groups. Peaks at 1616, 1440, 1400, and 1043 cm<sup>-1</sup> were preserved in TC600 but absent from TC600+NH<sub>4</sub> and TC600+P (after reaction with

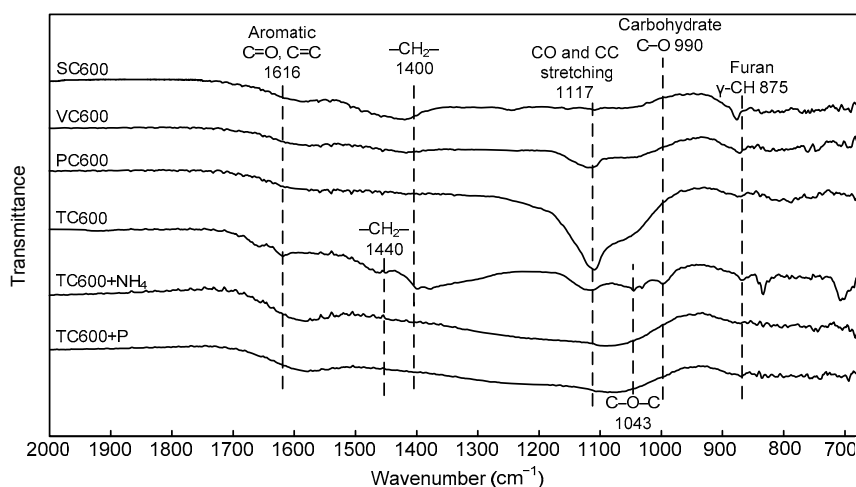


**Fig. 1** Fourier transform infrared (FTIR) spectra of biochar (600 °C) before and after reaction with ammonia or phosphate within the wavenumbers of 700–2000 cm<sup>-1</sup>

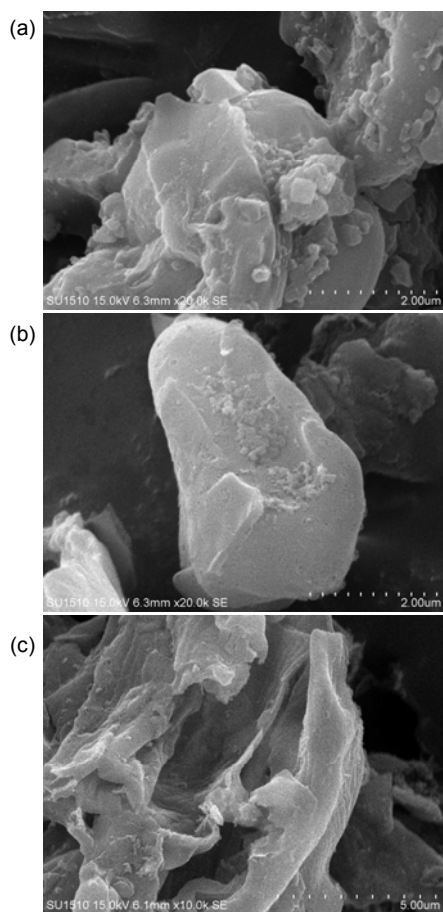


**Fig. 2** SEM images of TC600 before and after reaction with ammonia or phosphate  
(a) TC600; (b) TC600+NH<sub>4</sub>; (c) TC600+P

ammonia and phosphate, respectively), indicating that the functional groups (e.g., CH<sub>2</sub>, C–O–C) had reacted with NH<sub>4</sub>Cl and K<sub>2</sub>HPO<sub>4</sub>. Fig. 2 shows the SEM images of TC600 before and after ammonium and phosphate sorption. The SEM image of TC600 showed that the *T. dealbata* biochar had a smooth surface (Fig. 2a), which is consistent with the surface area measurements by the two different methods, indicating that its surface area was dominated by micropores. From the SEM images as shown in Figs. 2b and 2c, no significant differences were found between TC600, TC600+P, and TC600+NH<sub>4</sub>.

Glaser *et al.* (2002) assumed that formation of carboxylic groups by oxidation on the edges of the aromatic backbone of biochar was responsible for increased CEC. Some basic properties in the biochars can be attributed to the presence of basic functional groups (Pulido-Novicio *et al.*, 2001; Kameyama *et al.*,

2011). Chun *et al.* (2004) found a decrease in acidic functional groups and an increase in basic functional groups with increasing pyrolysis temperature. This phenomenon may have contributed to the lower CEC of biochar activated at higher temperatures. We found that the CEC of all of the biochar decreased when the activation temperature increased. In general, TC had the highest CEC of all the plant biochar at the same temperature. CEC decreased with increasing pyrolysis temperature, which might be induced by the thermolysis of cellulose and lignin at high temperatures and the presence of basic functional groups.

### 3.2 Sorption isotherms

The biochar of TC showed a very rapid increase in ammonium and phosphate sorption isotherms. The Freundlich and Langmuir isotherm models were used to describe the sorption of ammonium and phosphate into the biochar, which are expressed respectively as

$$Q_e = KC_e^N,$$

$$Q_e = Q_{\max} b C_e / (1 + b C_e),$$

where  $Q_e$  is the amount of adsorbate adsorbed at equilibrium (mg/g),  $C_e$  is the equilibrium concentration (mg/L),  $K$  is the relative adsorption capacity constant of the adsorbent (mg/g),  $N$  is the intensity of the adsorption constant,  $Q_{\max}$  is the monolayer maximum adsorption capacity (mg/g), and  $b$  is the affinity coefficient.

Figs. 3a–3c show the ammonium adsorption isotherms for SC, VC, TC, and PC at different temperatures. The corresponding Langmuir and Freundlich isotherm parameters and correlation coefficients are given in Table 2. The correlation coefficients ( $R^2$ ) of the Freundlich model are comparable to those of the Langmuir model, but the Freundlich model fits the data slightly better than the Langmuir model with the exception of *T. dealbata*. The Langmuir maximum capacity of TC700 was 17.579 mg/g, which is higher than that of other adsorbents for the sorption of ammonium from aqueous solutions. Based on the Freundlich affinity coefficient ( $K$ ), TC had a higher affinity for ammonium than SC, VC, and PC at the same temperature. This result is consistent with the maximum adsorption capacity. With the increase in temperature, the sorption capacity of all adsorbents increased.

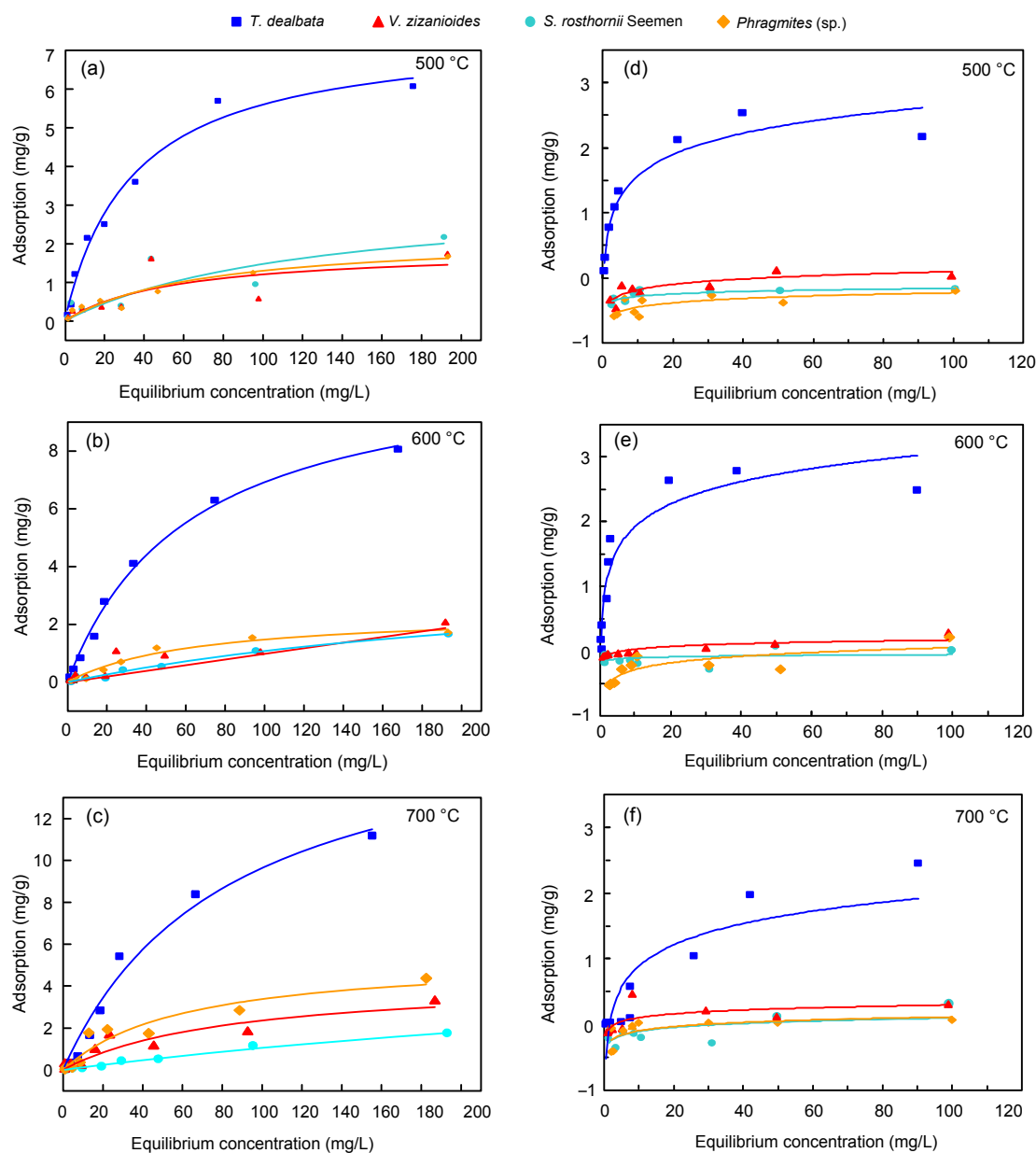


**Fig. 3 Sorption isotherms of ammonia (a, b, c) and phosphate (d, e, f) at different temperatures**  
(a) and (d) at 500°C, (b) and (e) at 600°C, (c) and (f) at 700 °C

Sorption isotherms of phosphate by biochar activated at different temperatures are presented in Figs. 3d–3f. TC700 had the greatest sorption capacity. Some isotherms of SC, VC, and PC showed negative values at lower concentration ranges, potentially because the biochar released some available *P* into the solution, resulting in lower initial concentrations than equilibrium concentrations. Hence, we analyzed Langmuir and Freundlich isotherm constants for TC

only (Table 3). The isotherm for phosphate fits the Langmuir model much better, with correlation coefficients ranging from 0.947 to 0.964. This result differs from previous reports showing that phosphate sorption fits the Freundlich isotherm better than does the Langmuir model because of phosphate precipitation (Yao *et al.*, 2011a). This discrepancy is possibly due to phosphate released from the biochar, which resulted in lower equilibrium values of adsorbed phosphate ( $Q_e$ ).

**Table 2** Parameters obtained from Langmuir and Freundlich isotherms for ammonium sorption on different biochars

Biochar	Freundlich model			Langmuir model		
	$K$ (mg/g)	$N$	$R^2$	$Q_{\max}$ (mg/g)	$b$ (L/mg)	$R^2$
SC500	0.088	0.598	0.697	3.31	0.008	0.625
SC600	0.022	0.850	0.984	7.43	0.002	0.982
SC700	0.020	0.854	0.994	6.61	0.002	0.993
TC500	0.636	0.458	0.925	7.49	0.030	0.980
TC600	0.487	0.561	0.958	11.2	0.016	0.993
TC700	0.483	0.636	0.937	17.6	0.012	0.975
VC500	0.104	0.517	0.587	1.87	0.018	0.520
VC600	0.070	0.634	0.865	3.12	0.008	0.847
VC700	0.162	0.567	0.888	4.36	0.012	0.852
PC500	0.110	0.519	0.986	2.21	0.014	0.957
PC600	0.107	0.550	0.897	2.43	0.016	0.958
PC700	0.253	0.547	0.907	5.43	0.016	0.899

SC: *S. rosthornii* Seemen; TC: *T. dealbata*; VC: *V. zizanioides*; PC: *Phragmites* sp.

**Table 3** Parameters obtained from the Langmuir and Freundlich isotherms for phosphate sorption by TC biochar\*

Biochar	Freundlich model			Langmuir model		
	$K$ (mg/g)	$N$	$R^2$	$Q_{\max}$ (mg/g)	$b$ (L/mg)	$R^2$
TC500	0.689	0.301	0.792	2.54	0.215	0.964
TC600	0.867	0.283	0.761	2.86	0.338	0.953
TC700	0.094	0.741	0.921	4.96	0.011	0.947

\* Data were not shown for SC, VC, and PC due to their low sorption capacity

### 3.3 Sorption of ammonium

Removal rates of ammonium (30 mg N/L) by TC500, TC600, and TC700 were (33.38±0.7)%, (37.28±2.2)%, and (37.84±3.2)%, respectively (Fig. 4a). The removal rates observed for TC were higher as compared to other adsorbents, indicating that TC has a greater ammonium sorption capacity. Chemical interaction may dominate physical sorption (different kinds of plant biochar at the same temperature) because the sorption capacity of TC was much greater than that of the other adsorbents at the same temperature despite the lower specific surface area of TC (Table 1).

It is widely recognized that biochar can be used as a soil amendment in agriculture. Most previous studies found that biochar addition increased soil CEC to retain nutrients (e.g., K, Ca, and  $\text{NH}_4^+$ ) (Glaser et al., 2002; Lehmann et al., 2003; Liang et al., 2006). The consistent correlation of ammonium sorption capacities and CEC of the tested biochar indicates that cation exchange dominated in ammonium removal (Ding et al., 2010). As predicted from

the previous observations, SC700, which has a lower CEC than VC700 and PC700, had the lowest removal rate despite having the largest surface area of the three biochars. This result confirms previous conclusions that, with the same activation temperature, CEC is the most important factor for ammonium sorption. However, with an increase in activation temperature for biochar from a given plant, both the surface area and ammonium removal rates increased, while CEC decreased, indicating that factors other than CEC, such as surface area, also affect sorption.

TC700 is the best material for ammonium removal (Fig. 4a) among the test biochar. However, TC600 had a similar ammonium removal rate to TC700, and the yield of TC600 was much higher than TC700 (Table 1). Although VC700 and PC700 had a greater specific surface area, they had a comparable yield and slightly lower removal rates for  $\text{NH}_4\text{-N}$ , as compared with TC600. In addition, extra energy is required to produce VC700 and PC700. Therefore, TC600 should be more economical for application of ammonium removal among the tested biochar.

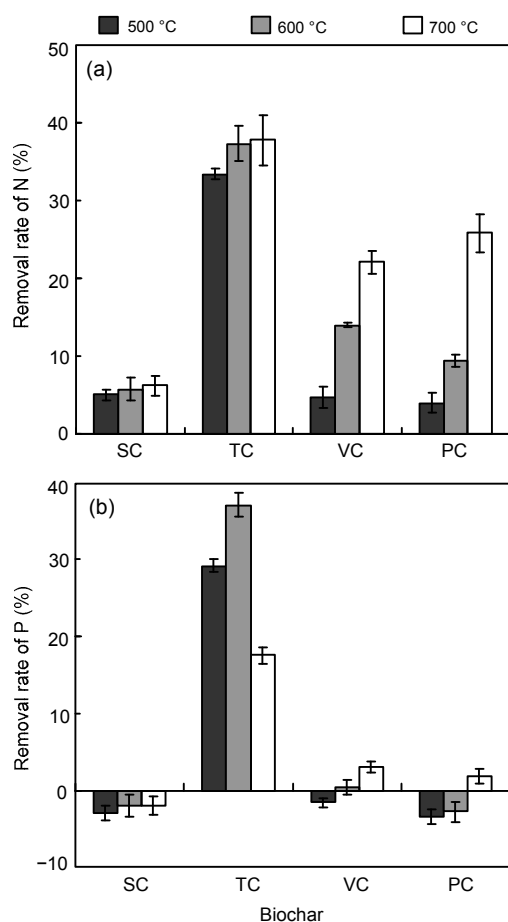


**Fig. 4 Comparison of ammonia (a) and phosphate (b) removal rates by different adsorbents**

Initial concentrations of N and P are both 30 mg/L. Data are expressed as mean $\pm$ SD,  $n=3$ . SC: *S. rosthornii* Seemen; TC: *T. dealbata*; VC: *V. zizanioides*; PC: *Phragmites* sp.

### 3.4 Sorption of phosphate

Sorption of phosphate from aqueous solutions is generally governed by the surface functional group, surface area of the adsorbent and metal-ion complex formation. Previous studies have demonstrated that the surface of the biochar is often negatively charged, making it repel negatively charged ions such as phosphate (Eberhardt *et al.*, 2006; Yao *et al.*, 2011a), suggesting that the sorption of phosphate via surface chemistry should be minimal. Similar to the above results for ammonium, TC, which has the lowest specific surface area, has the highest sorption capacity among all tested biochar pyrolyzed at the same temperature, suggesting that for different kinds of plant

biochar under the same temperature, the surface area was not the main factor in phosphate sorption.

Under alkaline conditions, the presence of Ca and Mg cations favors precipitation with phosphate (Gerritse, 1993; Arias *et al.*, 2001). For SC500, VC500, and PC500, with similar CEC and Ca content (Table 1), no removal of phosphate was observed, suggesting that Ca is insignificant in phosphate removal. This observation is consistent with Yao *et al.* (2011b), based on the X-ray diffraction (XRD) spectra of original and P-loaded biochar, that the precipitation of P with Ca may not be an important mechanism for phosphate removal because some Ca in biochar was present on its surface in the form of calcite, which has a low solubility, and Ca trapped inside the biochar could not be released into the solution. TC has the highest Mg content by a factor of three (Table 1). The greater phosphate removal by TC was probably due to its Mg content (Yao *et al.*, 2011a), which can precipitate phosphate in aqueous solutions.

TC had a greater phosphate sorption capacity than the other adsorbents but released some phosphate back into the solution (Fig. 4b), which is in line with Yao *et al.* (2011a). The removal value is in dynamic equilibrium between release and surface precipitation of P. High removal could be explained mainly by surface precipitation, and the available P may be responsible for phosphate release. TC samples that contained a higher available P had a higher P removal rate, indicating that surface precipitation of P is greater than the release of P in TC. On the contrary, in SC, VC, PC, the surface precipitation of P is smaller than the release of available P. With an increase in temperature from 500 to 700 °C, the amount of phosphate that SC, VC, and PC release back into the solution became negligible. Some adsorbents (VC700 and TC700) only removed a small amount of phosphate (3.03% and 1.80%, respectively). For biochar derived from a given plant, the surface area increased with the activation temperature, but the Mg content remained relatively constant (Table 1). Therefore, changes in phosphate removal are likely caused by interactions with the surface area, in the same plant biochar. The highest phosphate removal rate for TC, 38.12%, was observed when the biochar was activated at 600 °C. The same material activated at 700 °C had a lower phosphate removal rate, possibly because of the higher available P present in the



biochar (Table 1). Thus, TC600 is the best material for removing phosphate from aqueous solutions among the tested biochars.

#### 4 Conclusions

This study investigated the ability of biochar derived from four different phytoremediation plants to adsorb ammonium and phosphate from aqueous solutions. Physicochemical properties of the biochar, such as pH, surface area, and CEC, changed depending on the temperature at which the biochars were activated. In general, the removal rate rose as the activation temperature increased. Biochar derived from *T. dealbata* had the highest sorption capacity of all the plant biochar. Residue from *T. dealbata* can be used as a feed stock for biochar production. Considering the yields, high adsorption and energy cost, *T. dealbata* activated at a temperature of 600 °C (TC600) is the best adsorbent for removing phosphate and ammonium from aqueous solutions, which makes it of great interest in water eutrophication control. Though we performed the research using artificial wastewater, we believe the high removal efficiencies of ammonia and phosphate by biochars will provide more in-situ wastewater treatment opportunities.

#### Acknowledgements

The authors thank Dr. Erica HARTMANN (Arizona State University, USA) and Dr. Teng ZENG (Yale University, USA) for reviewing the manuscript.

#### Compliance with ethics guidelines

Zheng ZENG, Song-da ZHANG, Ting-qiang LI, Feng-liang ZHAO, Zhen-li HE, He-ping ZHAO, Xiao-e YANG, Hai-long WANG, Jing ZHAO, and Muhammad Tariq RAFIQ declare that they have no conflict of interest.

This article does not contain any studies with human or animal subjects performed by any of the authors.

#### References

- Abe, K., Ozaki, Y., 1998. Comparison of useful terrestrial and aquatic plant species for removal of nitrogen and phosphorus from domestic wastewater. *Soil Sci. Plant Nutr.*, **44**(4):599-607. [doi:10.1080/00380768.1998.10414483]
- Arias, C., Del Bubba, M., Brix, H., 2001. Phosphorus removal by sands for use as media in subsurface flow constructed reed beds. *Water Res.*, **35**(5):1159-1168. [doi:10.1016/S0043-1354(00)00368-7]
- Brix, H., 1997. Do macrophytes play a role in constructed treatment wetlands? *Water Sci. Technol.*, **35**(5):11-18. [doi:10.1016/S0273-1223(97)00047-4]
- Cao, X., Harris, W., 2010. Properties of dairy-manure-derived biochar pertinent to its potential use in remediation. *Bioresource Technol.*, **101**(14):5222-5228. [doi:10.1016/j.biortech.2010.02.052]
- Chun, Y., Sheng, G., Chiou, C.T., Xing, B., 2004. Compositions and sorptive properties of crop residue-derived chars. *Environ. Sci. Technol.*, **38**(17):4649-4655. [doi:10.1021/es035034w]
- Conley, D.J., Paerl, H.W., Howarth, R.W., Boesch, D.F., Seitzinger, S.P., Havens, K.E., Lancelot, C., Likens, G.E., 2009. Controlling eutrophication: nitrogen and phosphorus. *Science*, **323**(5917):1014-1015. [doi:10.1126/science.1167755]
- Demirbas, A., 2004. Effects of temperature and particle size on bio-char yield from pyrolysis of agricultural residues. *J. Anal. Appl. Pyrol.*, **72**(2):243-248. [doi:10.1016/j.jaap.2004.07.003]
- Ding, Y., Liu, Y.X., Wu, W.X., Shi, D.Z., Yang, M., Zhong, Z.K., 2010. Evaluation of biochar effects on nitrogen retention and leaching in multi-layered soil columns. *Water Air Soil Pollut.*, **213**(1-4):47-55. [doi:10.1007/s11270-010-0366-4]
- Eberhardt, T.L., Min, S.H., Han, J.S., 2006. Phosphate removal by refined aspen wood fiber treated with carboxymethyl cellulose and ferrous chloride. *Bioresource Technol.*, **97**(18):2371-2376. [doi:10.1016/j.biortech.2005.10.040]
- Gerritse, R.G., 1993. Prediction of travel times of phosphate in soils at a disposal site for wastewater. *Water Res.*, **27**(2):263-267. [doi:10.1016/0043-1354(93)90084-U]
- Glaser, B., Lehmann, J., Zech, W., 2002. Ameliorating physical and chemical properties of highly weathered soils in the tropics with charcoal—a review. *Biol. Fert. Soils*, **35**(4):219-230. [doi:10.1007/s00374-002-0466-4]
- Hossain, M.K., Strezov, V., Chan, K.Y., Ziolkowski, A., Nelson, P.F., 2011. Influence of pyrolysis temperature on production and nutrient properties of wastewater sludge biochar. *J. Environ. Manage.*, **92**(1):223-228. [doi:10.1016/j.jenvman.2010.09.008]
- Inyang, M., Gao, B., Yao, Y., Xue, Y., Zimmerman, A.R., Pullammanappallil, P., Cao, X., 2012. Removal of heavy metals from aqueous solution by biochars derived from anaerobically digested biomass. *Bioresource Technol.*, **110**:50-56. [doi:10.1016/j.biortech.2012.01.072]

- Kameyama, K., Miyamoto, T., Shiono, T., Shinogi, Y., 2011. Influence of sugarcane bagasse-derived biochar application on nitrate leaching in calcareous dark red soil. *J. Environ. Qual.*, **41**(4):1131-1137. [doi:10.2134/jeq2010.0453]
- Karaosmanoglu, F., İşigüç-Ergüdenler, A., Sever, A., 2000. Biochar from the straw-stalk of rapeseed plant. *Energy Fuels*, **14**(2):336-339. [doi:10.1021/ef9901138]
- Kumar, S., Loganathan, V.A., Gupta, R.B., Barnett, M.O., 2011. An assessment of U(VI) removal from groundwater using biochar produced from hydrothermal carbonization. *J. Environ. Manage.*, **92**(10):2504-2512. [doi:10.1016/j.jenvman.2011.05.013]
- Lehmann, J., da Silva, J.P.Jr., Steiner, C., Nehls, T., Zech, W., Glaser, B., 2003. Nutrient availability and leaching in an archaeological Anthrosol and a Ferralsol of the Central Amazon basin: fertilizer, manure and charcoal amendments. *Plant Soil*, **249**(2):343-357. [doi:10.1023/A:1022833116184]
- Liang, B., Lehmann, J., Solomon, D., Kinyangi, J., Grossman, J., O'Neill, B., Skjemstad, J.O., Thies, J., Luizão, F.J., Petersen, J., 2006. Black carbon increases cation exchange capacity in soils. *Soil Sci. Soc. Am. J.*, **70**(5):1719-1730. [doi:10.2136/sssaj2005.0383]
- Lu, Q., He, Z.L., Graetz, D.A., Stoffella, P.J., Yang, X., 2010. Phytoremediation to remove nutrients and improve eutrophic stormwaters using water lettuce (*Pistia stratiotes* L.). *Environ. Sci. Pollut. Res.*, **17**(1):84-96. [doi:10.1007/s11356-008-0094-0]
- Mohan, D., Pittman, C.U., Bricka, M., Smith, F., Yancey, B., Mohammad, J., Steele, P.H., Alexandre-Franco, M.F., Gómez-Serrano, V., Gong, H., 2007. Sorption of arsenic, cadmium, and lead by chars produced from fast pyrolysis of wood and bark during bio-oil production. *J. Coll. Interf. Sci.*, **310**(1):57-73. [doi:10.1016/j.jcis.2007.01.020]
- Pignatello, J.J., Kwon, S., Lu, Y., 2006. Effect of natural organic substances on the surface and adsorptive properties of environmental black carbon (char): attenuation of surface activity by humic and fulvic acids. *Environ. Sci. Technol.*, **40**(24):7757-7763. [doi:10.1021/es061307m]
- Pulido-Novicio, L., Hata, T., Kurimoto, Y., Doi, S., Ishihara, S., Imamura, Y., 2001. Adsorption capacities and related characteristics of wood charcoals carbonized using a one-step or two-step process. *J. Wood Sci.*, **47**(1):48-57. [doi:10.1007/BF00776645]
- Ravikovich, P.I., Neimark, A.V., 2001. Characterization of nanoporous materials from adsorption and desorption isotherms. *Coll. Surface A*, **187-188**:11-21. [doi:10.1016/S0927-7757(01)00614-8]
- Schollenberger, C., Simon, R., 1945. Determination of exchange capacity and exchangeable bases in soil-ammonium acetate method. *Soil Sci.*, **59**(1):13-24.
- Seo, B.S., Park, C.M., Song, U., Park, W.J., 2010. Nitrate and phosphate removal potentials of three willow species and a bald cypress from eutrophic aquatic environment. *Landscape Ecol. Eng.*, **6**(2):211-217. [doi:10.1007/s11355-009-0102-7]
- Uchimiya, M., Lima, I.M., Thomas Klasson, K., Chang, S.C., Wartelle, L.H., Rodgers, J.E., 2010. Immobilization of heavy metal ions (Cu<sup>II</sup>, Cd<sup>II</sup>, Ni<sup>II</sup>, and Pb<sup>II</sup>) by broiler litter-derived biochars in water and soil. *J. Agric. Food Chem.*, **58**(9):5538-5544. [doi:10.1021/jf9044217]
- Valipour, A., Kalyan Raman, V., Ghole, V.S., 2009. A new approach in wetland systems for domestic wastewater treatment using *Phragmites* sp. *Ecol. Eng.*, **35**(12):1797-1803. [doi:10.1016/j.ecoleng.2009.08.004]
- Valix, M., Cheung, W., McKay, G., 2004. Preparation of activated carbon using low temperature carbonisation and physical activation of high ash raw bagasse for acid dye adsorption. *Chemosphere*, **56**(5):493-501. [doi:10.1016/j.chemosphere.2004.04.004]
- Walton, K.S., Snurr, R.Q., 2007. Applicability of the BET method for determining surface areas of microporous metal-organic frameworks. *J. Am. Chem. Soc.*, **129**(27):8552-8556. [doi:10.1021/ja071174k]
- Wilkie, A.C., Evans, J.M., 2010. Aquatic plants: an opportunity feedstock in the age of bioenergy. *Biofuels*, **1**(2):311-321. [doi:10.4155/bfs.10.2]
- Xu, X., Cao, X., Zhao, L., Wang, H., Yu, H., Gao, B., 2013. Removal of Cu, Zn, and Cd from aqueous solutions by the dairy manure-derived biochar. *Environ. Sci. Pollut. Res.*, **20**(1):358-368. [doi:10.1007/s11356-012-0873-5]
- Yang, X., Wu, X., Hao, H., He, Z., 2008. Mechanisms and assessment of water eutrophication. *J. Zhejiang Univ.-Sci. B (Biomed. & Biotechnol.)*, **9**(3):197-209. [doi:10.1631/jzus.B0710626]
- Yao, Y., Gao, B., Inyang, M., Zimmerman, A.R., Cao, X., Pullammanappallil, P., Yang, L., 2011a. Biochar derived from anaerobically digested sugar beet tailings: characterization and phosphate removal potential. *Bioresource Technol.*, **102**(10):6273-6278. [doi:10.1016/j.biortech.2011.03.006]
- Yao, Y., Gao, B., Inyang, M., Zimmerman, A.R., Cao, X., Pullammanappallil, P., Yang, L., 2011b. Removal of phosphate from aqueous solution by biochar derived from anaerobically digested sugar beet tailings. *J. Hazard. Mater.*, **190**(1-3):501-507. [doi:10.1016/j.jhazmat.2011.03.083]
- Yuan, J.H., Xu, R.K., Zhang, H., 2011. The forms of alkalis in the biochar produced from crop residues at different temperatures. *Bioresource Technol.*, **102**(3):3488-3497. [doi:10.1016/j.biortech.2010.11.018]
- Zhao, F., Yang, W., Zeng, Z., Li, H., Yang, X., He, Z., Gu, B., Rafiq, M.T., Peng, H., 2012. Nutrient removal efficiency and biomass production of different bioenergy plants in hypereutrophic water. *Biomass Bioenergy*, **42**:212-218. [doi:10.1016/j.biombioe.2012.04.003]